Engineering

Mechanical Engineering fields

Okayama University *Year* 2007

The Convective Instability in a Microemulsion Phase-Change-Material Slurry Layer

Hideo Inaba
Okayama University

Chuanshan Dai
Tianjin University

Akihiko Horibe
Okayama University

The Convective Instability in a Microemulsion Phase-Change-Material Slurry Layer*

Hideo INABA**, Chuanshan DAI*** and Akihiko HORIBE**

In the present experimental study, the stability of Rayleigh-Bénard convection has been investigated in rectangular enclosures filled with microemulsion Phase-Change-Material (PCM) slurry. The PCM slurry exhibited a pseudoplastic non-Newtonian fluid behavior. Hysteresis in convection was clearly observed while the PCM were in a solid phase and in phase changing. The critical Rayleigh number decreases with the PCM mass concentration while the PCM is in phase changing. The fluid temperature at the center of the enclosure showed a time-dependent oscillation during the transition from a heat conduction state to a convection state. The maximum Nusselt number has been observed for all of the slurries while the heating plate was controlled at a temperature that most of PCM was in phase changing.

Key Words: Rayleigh-Bénard Convection, Microemulsion, Phase Change Material, Convective Instability, Subcritical Convection, Hysteresis

1. Introduction

Rayleigh-Bénard convection is a classical problem in fluid dynamics and pattern formations in nonlinear systems. It has been extensively studied in the last four decades since the monograph dedicated by Chandrasekhar[1]. The previous researches on this problem can be classified into a number of platforms, e.g. the flow pattern formation and its stability, the chaos and its route to turbulence (for comprehensive reviews, see Davis[2]; Mannelille[3]; Getling[4]), the real boundary effects (Cerisier et al.[5]; Howle[6]), and more recently the suppression and the active control of thermal convection (Tang et al.[7]; Howle[8]) and others. The linear and the weakly nonlinear stability theories are still the main methods being used for the analysis of a marginal stability or the onset of thermal convection theoretically. However, on considering the fluctuations of fluid properties such as viscosity, thermal diffusivity with temperature or the non-Boussinesq effects on the stability of thermal convection for a complex fluid, the weakly nonlinear analyses, if possible, are still very complicated (Chung and Chen[9]). In this case, a simplified model is encouraged. Nevertheless, this cannot be achieved without the careful guidance from the results of an experiment.

In the last decade, the complex fluids have been attracting many researchers' attention. Because the self-assembly or the self-organization feature in the microstructure of these fluids is similar to those of biofluids having multi-functions in supporting the life of a living body (Lehn[10]; Ikkala & Brinke[11]). Microemulsion is a kind of ternary water-oil-surfactant mixtures, and holds very complex physical and rheological properties due to the kinetics of phase separation and self-assembling morphology induced by colloidal particles (Chen & Ma[12]; Yamamoto & Tanaka[13]). If the oil component is replaced by phase change material (PCM), the mixture suspensions can have a great potential to be used in heat transfer enhancement, heat storage and fluid transportation (Inaba 2000[14]; Choi, Cho & Lorsch[15]; Inaba & Morita[16]), because of the absorption or emission of a large amount of latent heat with the melting or solidification of the PCM in the slurries when they are

* Received 12th March, 2003 (No. 03-4030)

** Department of Mechanical Engineering, Faculty of Engineering, Okayama University, 3-1-1 Tsushima-naka, Okayama 700-8530, Japan. E-mail: inaba @mech.okayama-u.ac.jp (H. Inaba)

*** Tianjin Geothermal Research and Training Center, Tianjin University, 300074, People's Republic of China

subject to heating or cooling, respectively. In addition to some heat transfer characteristics in the thermal applications as discussed in the previous studies (Inaba, Dai & Horibe 2003[17]; Inaba, Dai & Horibe 2002[18]), some interesting phenomena in the fluid dynamics of Rayleigh-Bénard convection had also been observed.

Except for the Boussinesq Newtonian fluids, the theoretical predictions of the critical Rayleigh number, generally, do not agree with those obtained from the experiments, or even have an opposite trend. The reasons can be explained by the fact that the boundary conditions in a theoretical modeling are too simple and too universal to be realized in an experiment. On the other hand, the variations in thermal or rheological properties of a real fluid with temperature make it difficult to be dealt with in a theoretical analysis. The purpose of the present study is to show experimentally the onset of Rayleigh-Bénard convection for the microemulsion PCM slurry and some characteristics in convective stability and heat transfer. The focus is on the hysteresis phenomenon in convection and the transition characteristics from no-motion conduction state to convective state. The PCM mass concentration of the microemulsion slurry is varied from the maximum original 30% to the dilute 5%. The rectangular enclosure height is varied from 5.5 mm to 24.6 mm. Most of our experiments are concentrated on the enclosure with the lowest height of 5.5 mm, and the slurry with a PCM mass concentration of 20%.

2. The Properties of Microemulsion PCM Slurries

The external appearance of the microemulsion PCM slurry used in the present experiment is shown in Fig. 1. It has a white color and fluidity. It is well known that the main barriers for preventing the microemulsion PCM slurry from a possible real application in engineering are the stratification and/or the agglomeration due to a large size of the PCM particles in the slurry. But, these problems can be significantly improved simply by reducing the size of particles. The present technology can make the diameter of the PCM particles in less than one micrometer, which are much smaller than those used in the past, for instance, by Datta, Sengupta & Singh[19]. The PCM particle diameter distribution used in the present experiments ranged from 0.1 to 1.2 μm, and the bulk averaged diameter was about d_m= 0.51 μm, as shown in Fig. 2. By diluting the original microemulsion PCM slurry with distilled water, the less concentrated PCM slurries can be made. A 200 ml separatory funnel was used for checking if any stratification of the PCM slurry occurred. The slurries both before and after heated have been inspected. The results showed no evidences of any stratification. Figure 3 shows the main thermal properties of the microemulsion PCM slurry at a mass concentration of 20%. Except for the specific heat capacity that was measured by the differential scanning calorimetry (DSC), all of the other properties were measured at a thermal steady state.

As shown in Fig. 3, the thermal properties show dramatically fluctuations with temperature in the range from 40°C to 50°C. The density decreases rapidly with increasing temperature. The volumetric expansion coefficient in Fig. 3(c) shows a similar pattern with the specific heat in Fig. 3(d) in which a local maximum exists at a temperature of approximately 46°C. However, while the PCM particles are in a liquid phase, the volumetric expansion coefficient is smaller than that of water in the temperature range from about 50°C to 60°C. The measured data of density by a pycnometer show almost the same as the volumetric expansion coefficient. The phase changing region of the PCM almost covers the temperature range from 40°C to 50°C. Hence, the temperature range in the experiments was classified into three subregions according to the phase of PCM particles,

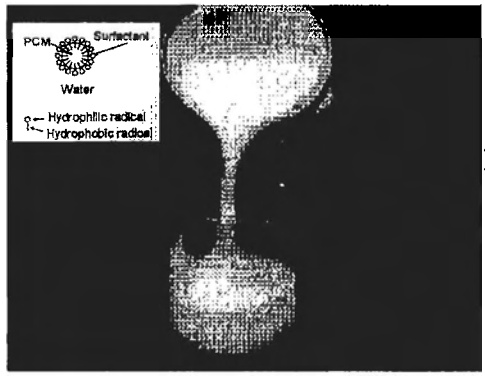

Fig. 1 The external appearance of the microemulsion PCM slurry

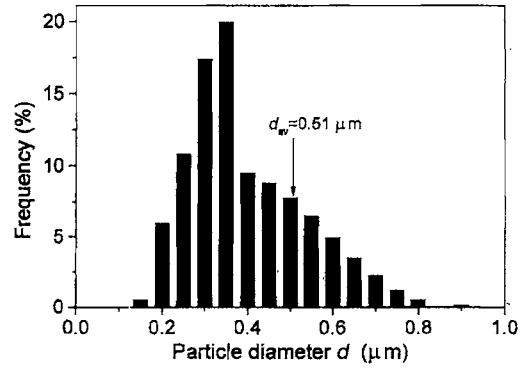

Fig. 2 Microemulsion particle size distribution

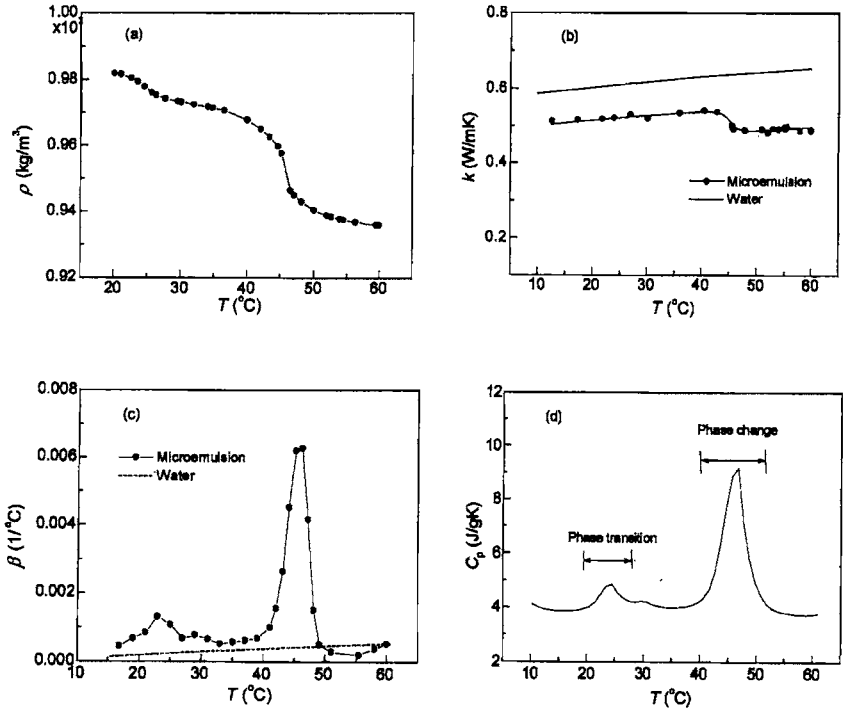

Fig. 3 Physical properties of microemulsion slurry (C=20 mass%) : (a) density, (b) thermal conductivity, (c) volumetric thermal expansion coefficient, (d) apparent specific heat capacity detected by DSC

which were the solid phase region (T<40°C), the phase changing region (40°C< T <50°C) and the liquid phase region (T>50°C). The thermal conductivity was measured by the experimental apparatus itself and will be described in the later section. The PCM particles have a lower thermal conductivity than that of water.

Two types of rheometers have been used for measuring the viscosities of the microemulsion PCM slurries. One was a rheometer Model DV-III, a product of Brookfield. It was a cone-and-plate type with a cone angle of 0.8°, and its sample volume 0.5 ml. The other was a rotating cylinder type. The inner rotating cylinder had a diameter of 25 mm and a length 90 mm. The gap between the inner and outer cylinders was 1.5 mm. The sample volume was 20 ml. However, the measured data using the cone-and-plate configuration was not stable. On the other hand, all of the data measured using the rotating cylinder viscosimeter were stable and repeatable. Hence, the rotating cylinder type viscosimeter was preferred. A systematic experiment has not been conducted on the threshold of flow stability problem for these two types of rheometers. More recently, there appears an increasing research interest on this problem for both the two above-mentioned configurations in polymer solutions or viscoelastic fluids (Rothstein & Mckinley[20] ; Ali et al.[21]).

The uncertainties for the measured properties are as follows. The pycnometer had an accuracy of within $\pm 5.0\times10^{-4}$ kg/m³ in density measurement. For the measurement of the apparent specific heat, the DSC was used, and the calibrated data using water indicated that the standard deviation was of ±1.5%. The volumetric expansion meter had a measuring accuracy of ±0.02%. The viscosity for water measured by the rotary cylinder rheometer was represented with a standard deviation of ±2.0% in agreement with the reference values.

The measured stress rates against a strain rate showed that the slurry followed a power law model of pseudoplastic non-Newtonian fluids. Figure 4(a) and (b) show the pseudoplastic fluid index n and viscosity consistency K, respectively. The apparent viscosity is higher for the PCM in a solid phase (T< 40°C) than that for the PCM in a liquid phase (T> 50°C). In other words, the viscosity is decreased with melting of the PCM particles. The more diluted or the less concentrated PCM slurry has a lower viscosity at the same strain rate.

3. Experimental Setup and Procedure

As depicted in Fig. 5, the present experiments were conducted in a horizontally placed rectangular enclosure, which consisted of a transparent acrylic side-wall frame (10 mm thick) ⑬ and two copper

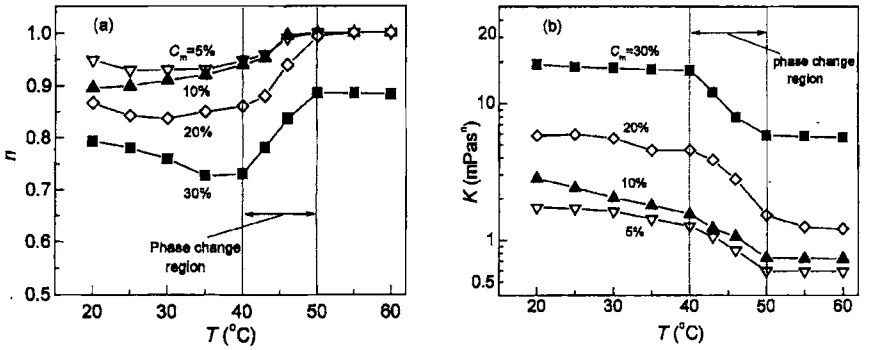

Fig. 4 Rheological properties of microemulsion slurries with different concentrations (a) pseudoplastic fluid indexes, (b) consistent viscosity.

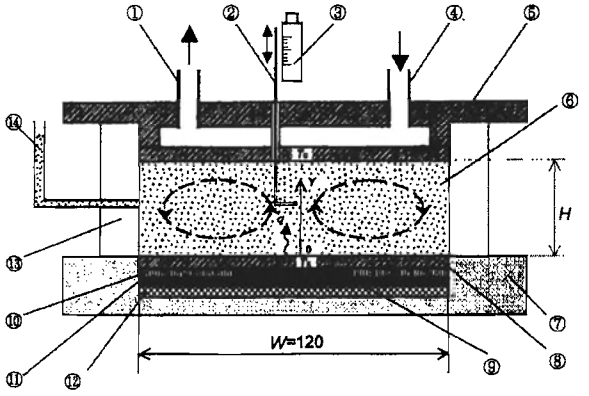

Fig. 5 Schematic of experimental apparatus: ① Outlet of cooling water; ② Traversing thermocouple; ③ Micrometer; ④ Inlet of cooling water; ⑤ Cooling copper plate; ⑥ PCM slurry; ⑦ Bakelite backing plate; ⑧ Heating copper plate; ⑨ Heat flux sensor; ⑩ Packing film; ⑪ Film heater; ⑫ Thermal insulator; ⑬ Acrylic supporter; ⑭ Reservoir; • Thermocouple

plates (10 mm thick) ⑤ and ⑧. The copper plates were fitted to the top and bottom ends of the frame. The temperature of the top cooling copper plate was maintained by circulating the cooling brine through a water bath. A 0.7 mm thick electric film heater ⑪ was mounted to the bottom of the lower heating copper plate. A 0.2 mm thick and 50 mm in square film heat flux sensor ⑨, which had a measuring accuracy of 1.0 W/m^2, was inserted between the heating copper plate and the film heater. The thermal resistance of the film heat flux sensor is about 0.000 5°C/(W/m^2). A packing film ⑩ of the same material as the heat flow sensor was mounted around the heat flux sensor in order to compensate the equal heat flux to its sensor. The backside of the film heater was covered with 5 mm thick foamed thermal insulating material ⑫. A 15 mm thick bakelite plate ⑦ was mounted below the thermal insulating material. The whole test section was covered with 50 mm thick foamed thermal insulating material. A glass pipe of 8.0 mm in an inner diameter ⑭ was connected with the test section as an expansion reservoir of the microemulsion slurry. The mean temperatures of the heating and cooling copper plates were measured, respectively, by six T-type thermocouples with a diameter of 0.1 mm, and two of them were buried in the middle and four of them were located around of the heating or the cooling plate. All the thermocouples were calibrated carefully and individually using constant-temperature water bath, and their accuracy after calibrated was about ±0.2°C. The temperature of the heating copper plate was adjusted by controlling the input electric power of the heater. The height of the rectangular enclosure H or the aspect ratio AR can be varied by selecting a suitable acrylic plate side-wall frame ⑬. Two T-type thermocouples supported by a 1.06 mm in an outer diameter and 0.18 mm thick stainless pipe ② were installed to measure the vertical temperature distribution at the center of the enclosure. Their positions were controlled with a micrometer ③.

Since the microemulsion PCM slurry was not transparent, the visualization method of flow pattern such as shadowgraph is not suitable for the present case. A *Nu-Ra* plot method was used for determining if convection had occurred from a no-motion heat conduction state. Therefore, the heat transfer measurement is crucial and, the errors due to any uncertainties should be minimized. The main consideration in the heat transfer measurement was the heat-loss to the surrounding of the experimental apparatus by heat conduction, even though the experimental apparatus was thermally insulated. In order to estimate the heat-loss from the experimental apparatus, firstly the apparatus was calibrated by turning it upside down under the top heating and bottom cooling conditions and running heat conduction experiment at a steady state using water as a test fluid. The repeated experiments with different electric power inputs and temperature differences between the top heating cop-

per plate and the room showed that the heat-loss was approximately a linear function of the temperature difference. The linear function obtained was used as a correction for the convective heat transfer experiments.

The definition of Nusselt number is as follows,

$$Nu=\frac{Q_{corr}H}{k(T_H-T_C)}, \quad (1)$$

where Q_{corr} is the corrected heat flux through the fluid layer calculated by using the following equations, H is the depth of fluid layer. T_H and T_C are, respectively, the top and bottom plate temperatures. k is the thermal conductivity at mean temperature of $(T_C+T_H)/2$.

$$Q_{corr}=Q-Q_{loss}, \quad (2)$$

$$Q_{loss}=a+b(T_H-T_{room}), \quad (3)$$

where a, and b were curve fitting constants obtained by using the calibration data. The corrected part of heat Q_{loss} was in general less than 5% of the total heat input Q in the case of water experiment and air-conditioned room temperatures. The measured thermal conductivities of water by using the method described above were in agreement with the reference values of water with a standard deviation of ±1%. The thermal conductivity of the microemulsion slurry was measured by the calibrated experimental apparatus in the same way. The top cooling plate temperature was maintained by circulating the cooling brine through a water tank, which had a temperature accuracy of ±0.01°C~±0.1°C in control. The bottom heating plate temperature, the heat flux through the fluid layer, the test fluid temperature at the center of enclosure and the ambient temperature were monitored in every 10 seconds. The whole test system was evaluated at a thermal steady state condition if the heating plate temperature fluctuation was within ±0.05°C in an hour. While the system was confirmed at a thermal steady state, the vertical fluid temperature distribution in the middle of the enclosure was measured by traversing the two thermocouples ② as illustrated in Fig. 3 from the bottom to the top of the test fluid layer and, its position can be controlled within an accuracy of $\pm 5.0\times10^{-3}$ mm. The time step of 10 seconds used in monitoring was long enough for waiting a next response of thermocouple, and short than the time duration required for a temperature perturbation transferring through the whole fluid layer. The thermal diffusivity of the microemulsion PCM slurry ($\approx 1.35\times10^{-7}$ m^2/s) was a little bit lower than that of water. Therefore, the time period ($=H^2/a$) required for transferring the temperature perturbation through the whole test fluid layer was about 230 s for the enclosure with the lowest height 5.5 mm and about 4 500 s for the enclosure with the height 24.6 mm. Those time periods were, respectively, in about one and two orders longer than the data acquisition time step of 10 s. Hence, the data acquisition in every 10 seconds was capable of responding a temperature variation at the threshold of flow instability.

The effect of boundary conditions on the onset of Rayleigh-Bénard convection was investigated by Cerisier et al.[5] and latter by Howle[6] for the actively controlled case. As pointed out by Cerisier et al., the critical Rayleigh number will remain to be 1 708 for an infinite horizontal water layer confined between two copper plate boundaries. Because the thermal conductivity ratio of copper to water lies in the order of 500 that the temperature disturbance vanishes and the temperature of the boundaries is uniform. In finite enclosures, the critical Rayleigh number should be higher than that of in an infinite horizontal fluid layer configuration due to the effects of side walls. But, the critical Rayleigh number decreases rapidly with an increase in the aspect ratio (Width/Height) (Davis[22]; Stork & Müller[23]. The Rayleigh-Bénard convection in an enclosure with thermal insulated sidewalls has a lower critical Rayleigh number compared with perfect heat conduction sidewalls. Based on the analysis mentioned above, the critical Rayleigh numbers for water in the enclosures used in the present experiments should be consistent with those of previous works, which lie between 1 708 to about 2 100.

4. Onset of the Microemulsion PCM Slurries without and with Phase Changing

4.1 PCM in solid phase

While the PCM in the microemulsion is in a pure solid or liquid phase, the rheological properties show that it has no much different from a normal pseudoplastic non-Newtonian fluid. Ozoe and Churchill[24] numerically analyzed the neutral stability problem for a pseudoplastic non-Newtonian fluid. They showed that the critical Rayleigh number decreased with a decrease in pseudoplastic index n. This was in general agreement with the prior published but very limited experimental data obtained by Tien et al.[25], even the numerical results did not fit to those data very well. However, the idea of finding the critical Rayleigh number without referring to its flow patterns was criticized by Parmentier and Turcotte[26] and, they pointed out that thermal instabilities in a non-Newtonian fluid layer, unlike those in a Newtonian fluid layer, were inherently nonlinear because of the nonlinearity of the viscosity law. There were very few research works published on this problem thereafter. Solomatov[27] proposed a correlation for predicting the critical Rayleigh number of a non-

Newtonian fluid. But, the verification of the proposed correlation still was based on very limited experimental data of Tien et al.[25]

The microemulsion PCM slurry used in the present experiment showed a quite different thermal instability from those described above while heating from the bottom and cooling from the top. The experiments were conducted by fixing the cooling plate temperature at about 30°C for the PCM in a solid phase and, the heating plate temperature was varied by increasing the electric power input of the film heater in step. Figure 6 shows the variation of Nusselt number with Rayleigh number for the enclosure height of 5.5 mm or the aspect ratio of 21.8 and for the slurries with various PCM mass concentrations. As shown in Fig. 6, while the initial condition is in a motionless conduction state, no convection could be induced by increasing the lower heating plate temperature up to 35°C. Thus, the critical Rayleigh number for the microemulsion PCM slurry was much higher than those obtained in the previous experimental or theoretical studies. The definition of Rayleigh number is as follows,

$$Ra=\frac{\rho_0 g\bar{\beta}(T_H-T_C)H^{2n+1}}{Ka^n} \quad (4)$$

where n, K are the pseudoplastic fluid index and viscosity consistency, respectively. g is the gravity acceleration. ρ_0 is the density at temperature T_C. While deriving the thermal diffusivity a, the reference density, thermal conductivity and specific heat are taken the values at a mean temperature of $(T_C+T_H)/2$. Since the density and apparent specific heat of the PCM slurry are strong functions of temperature, they were particularly considered in the definition of Rayleigh number. The integral averaged

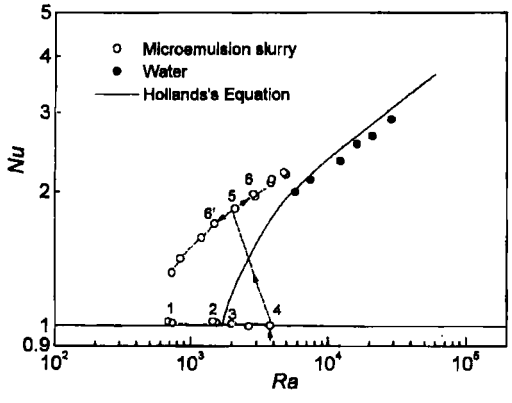

Fig. 6 Nusselt number vs Rayleigh number for $AR=21.8$ ($H=5.5$ mm) and $C_m=20\%$. The PCM in the slurry is in solid phase. The series numbers from 1 to 6 connected by the dash line represent the data obtained in sequence from a low to a high heating rate

volumetric expansion coefficient $\bar{\beta}$ from T_C to T_H was applied. Other thermal properties in the definition of Ra number are the values at a mean temperature of $(T_C+T_H)/2$.

It should be stressed that by taking a different reference thermal property may lead to a different interpretation about the behavior of the critical Rayleigh number and Nu-Ra plot. This was particularly pointed out by several authors[28]-[30]. The definition of Rayleigh number in the present paper was based on the following considerations. For a fluid with a large density variation in temperature, the integral averaged volumetric expansion coefficient would be better than the arithmetic averaged at a mean temperature $(T_C+T_H)/2$. This can be easily demonstrated using the expression of buoyancy force. However, the density used in deriving the thermal diffusivity was taken the value at reference temperature of $(T_C+T_H)/2$. The apparent specific heat for the PCM slurry was divided into two parts. One is the sensible heat and the other latent heat. Since the sensible heat at temperature while the PCM beginning to melt (±40°C) is approximately equal to that while all the PCM having melted (≈50°C), the reference specific heat was taken the value at a temperature of top cooling plate T_C. The influence of latent heat on natural convection was considered separately by introducing a modified Stefan number, as described latter.

The experimental results show that convection could not be induced for the case $C_m=30\%$ and $AR=21.8$, the fluid layer remains at a steady thermal conduction state for the heating plate temperature up to 40°C. For the less concentrated PCM slurry, such as $C_m=20\%$, 10% and 5%, the hysteresis phenomenon is very obvious in the Nu-Ra plot. Such jump increase in Nusselt number with respect to Rayleigh had been observed by some authors, such as Richter et al.[31] for the fluid with large variation in viscosity, and Thess and Orszag[32] for Bénard convection with surface-tension-driven force. It has not been observed in the PCM microemulsion slurry with Rayleigh-Bénard configuration. The physical mechanism about the hysteresis phenomenon in PCM slurry is not yet clear, because the present case does not seem to link directly with the two cases above. The series number from 1 to 6 in Fig. 6 means in sequence from a low to a high heating rate. After the convection sets in, the convective state will remain even at a small temperature difference between the heating and cooling plates. The arrow from point 5 to point 6′ represents the direction of decreasing the heating rate while the convective state is already existent in the enclosure. As a reference, the data of water were also measured

(solid circle). The solid line corresponds to the Hollands's correlation for an infinite two horizontal plates configuration (Hollands et al.[33]). Figure 7 shows the dynamic developing process of the heating plate temperature T_H, the fluid temperature at the center T_{mid}, and the input heating power q. By increasing the heating rate, the hot plate temperature increased at the beginning from point 3 to point 4, but dropped down soon after from 4 to 5, as seen in Fig. 7. The fluid temperature at the center showed a high frequency oscillation during the transition period from a motionless conduction state to a convection state, and finally evolved into a low frequency oscillation in a steady convection state. The vertical temperature distribution (Y direction in Fig. 3) at the center of the enclosure for each thermal steady state is shown in

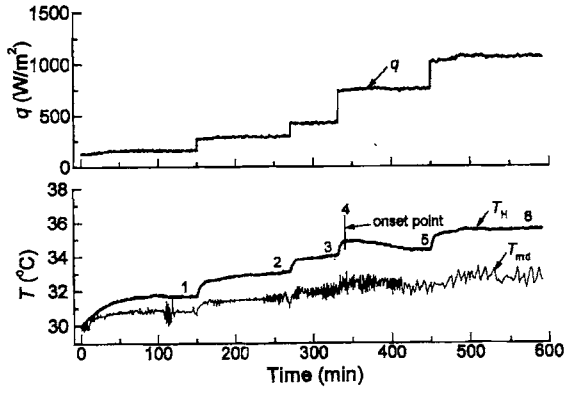

Fig. 7 Time recording of the heat flux q, the temperature of bottom heating plate T_H and the fluid temperature at the center T_{mid} for AR=21.8 (H=5.5 mm) and C_m=20%. The PCM in the slurry is in solid phase. For the caption of series numbers from 1 to 6 see Fig. 6

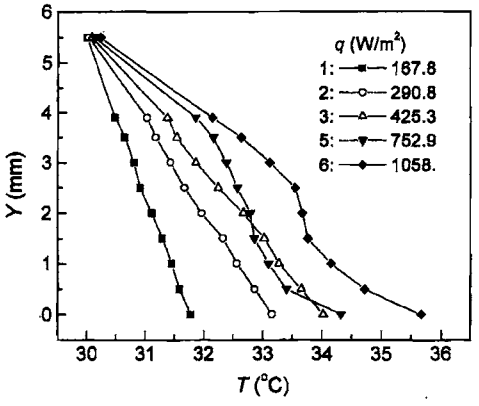

Fig. 8 Vertical temperature distribution in the middle of enclosure at the thermal steady conditions for AR =21.8 or H=5.5 mm, C_m=20%, and the PCM in the slurry is in solid phase. (see caption in Fig.s 6 and 7 for the series numbers)

Fig. 8, which can be used to confirm the fluid layer in a conduction-dominated or convection-dominated state. Lines 1 and 2 in Fig. 8 show clearly a linear relationship corresponding to a thermal conductive state. Line 3 is slightly departure from a linear relationship and, lines 4 and 5 are totally curved, which suggests that the fluid layer was dominated by natural convection.

4.2 PCM in phase changing

The influence on the onset and flow patterns due to the variations in fluid properties with temperature has been an academic research interest for several decades. The most extensively studied seems on the effect of viscosity fluctuation with temperature, since the viscosity plays an important role in flow pattern formation and instability (Busse[34]). Both theoretical and experimental studies can be available (Richter et al.[31]; Booker[35]; Stengel et al.[36]; Ogawa et al.[37]). The study on this problem was also motivated by the understanding of the Earth's upper mantle formation and evolution process, in which both Newtonian and non-Newtonian fluids was concerned (Christensen[38]). As pointed out by Solomatov[27], the onset of convection in power-law fluids is always a finite amplitude instability because the viscosity depends on the amplitude of initial perturbations and goes to infinity when the perturbations approach zero. However, little attention has been paid on the effect of remarkable temperature-dependent specific heat capacity and density on the onset of convection and the instability for both Newtonian and non-Newtonian fluids. There are already the difficulties in an analysis even for a Boussinesq fluid. In addition, the lack of experimental data is one of the main reasons for preventing someone from giving a reasonable theoretical model.

For C_m=30%, the convection could be induced with a small temperature difference, the hysteresis had not been detected while the PCM was in phase changing. However, it was clearly observed for the cases C_m=20%, 10% and 5%. Figure 9 shows the Nu-Ra plot for C_m=20% and for H=5.5 mm or AR= 21.8. By replacing the reference specific heat at temperature T_c with the apparent specific heat at a mean temperature $(T_c+T_H)/2$ in the definition of Rayleigh number, the open circles change to solid circles, as shown in Fig. 9. The decrease in Nusselt number (9→ 10) has been observed while the heating plate temperature is over about 46°C, which is the temperature for the slurry having a local maximum apparent specific heat capacity.

Figure 10 shows the time recording of heating rate q, the temperatures of the heating plate T_H and of the fluid at the center of enclosure T_{mid}. The two graphs at the bottom of Fig. 10 are the two figure

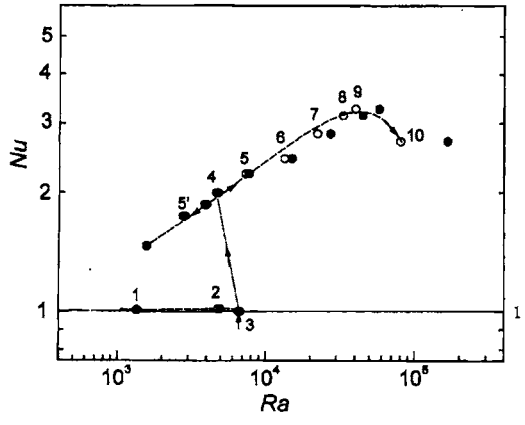

Fig. 9 Nusselt number vs Rayleigh number for AR=21.8 (H=5.5 mm) and C_m=20%. The PCM in the slurries is in phase changing. The series numbers from 1 to 10 represent the data obtained in sequence from a low to a high heating rate. Open circles are for the case using the reference specific heat without latent heat, and solid circles are for the case using the reference specific heat with latent heat.

zooms for the onset point indicating the start of convection (bottom left), and the deflection point indicating the rapidly drop in convective heat transfer coefficient (bottom right). The remarkable time-dependent fluid temperature at the center of the enclosure near the onset condition is also shown clearly in Fig. 10, which is the same as expressed in the preceding section for the PCM in a solid phase. The series number from 1 to 10 represents the increase in heating rate through the test fluid layer, and point 3 corresponds to the onset point. Point 4 is the first point evolved from a motionless state to a steady convective state. If the heating rate was decreased rather than increased herein, the convective state would be remained even for a small temperature difference shown from 4 to 5′ in Fig. 9. The mechanism for the appearance of deflection point is complicated, since it involves with a secondary instability problem. But, it is almost clear that the flow pattern is quite unstable in this temperature range (from 46°C to 50°C).

Figure 11 shows the vertical temperature distribution of the test fluid in the middle of the enclosure at a thermal steady condition corresponding to Fig. 10. It is confirmed that the first two conditions were at a heat conduction state and, the last had a jump in heating plate temperature resulting in a rapid drop in heat transfer coefficient or Nusselt number as depicted in Fig. 9. There are probably two reasons for the jump in heating plate temperature or the decrease in Nusselt number. One is due to the latent heat or the

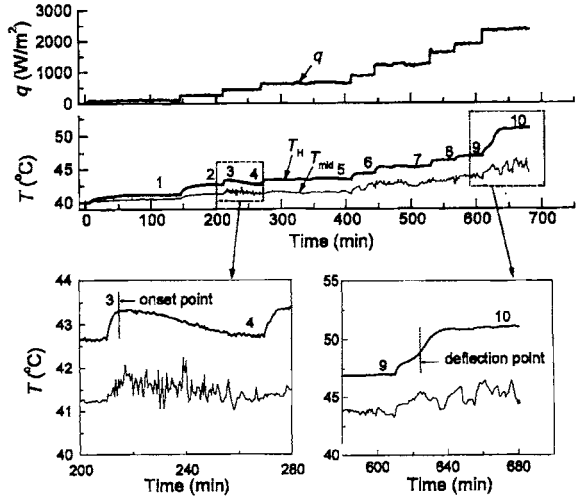

Fig.10 Time recording of the heat flux q (top), the temperature of the heating plate T_H (middle) and the fluid temperature at the center T_{mid} (middle) for AR=21.8 (H=5.5 mm) and C_m=20%. The PCM in the slurry is in phase changing. The left and right figures at the bottom represent, respectively, the figure zooms for the onset point and the deflection point in the regimes shown in the dash line boxes (middle). For the caption of series numbers from 1 to 10 see Fig. 9

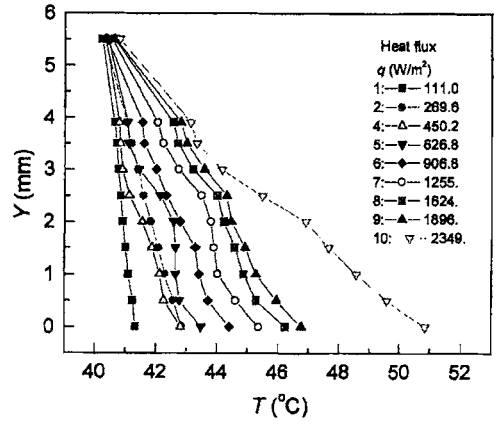

Fig. 11 Vertical fluid temperature distribution in the middle of enclosure at the thermal steady conditions for AR=21.8 (H=5.5 mm) and C_m=20%. The PCM in the slurry is in phase changing. For the caption of series numbers from 1 to 10 see Fig 9

apparent specific heat of the PCM slurry. While the heating plate temperature increasing from 46°C to 50°C, the apparent specific heat decreases rapidly, as shown in Fig. 3(d). The second is due to the density variation in temperature. Because the bulk average temperature is rising to about 45°C, at which the fluid density decreases rapidly as shown in Fig. 3(a), the actual amount of slurry involving in convective heat

transfer decreases. The deflection point became less and less obvious with a decrease in PCM mass concentration (from 30% to 5%).

4.3 PCM in a liquid phase

While the PCM in the microemulsion slurry is in a liquid phase, the experiments were conducted by fixing the cooling brine at 50°C and, the heating plate temperature was varied up to 60°C by controlling the heating rate. The *Nu-Ra* plot shown in Fig. 12 indicates that no convection was induced for the microemulsion PCM slurry with the mass concentrations of 20%. This was confirmed by the measured vertical temperature distribution in the middle of enclosure, as shown in Fig. 13. The critical Rayleigh number seems to be higher for the PCM in a liquid phase than those for the PCM in a solid phase and in phase changing, or that the critical Rayleigh number increases with melting of PCM in the slurry according to the measured data. This could be possibly contributed to the difference in the self-assembly morphology of the PCM particles while they are in a solid or liquid phase.

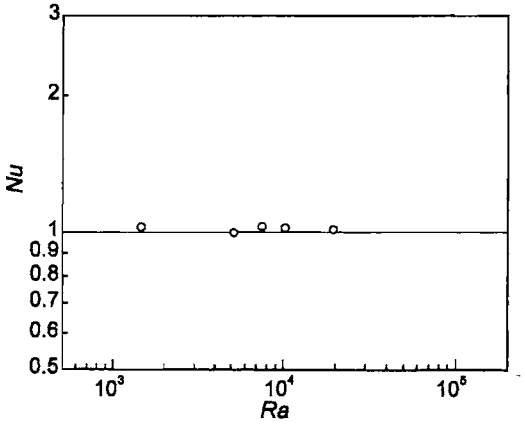

Fig. 12 Nusselt number against Rayleigh number at thermal steady state conditions for AR=21.8 or H=5.5 mm in the slurry with a mass concentrations of 20%. The PCM is in liquid phase.

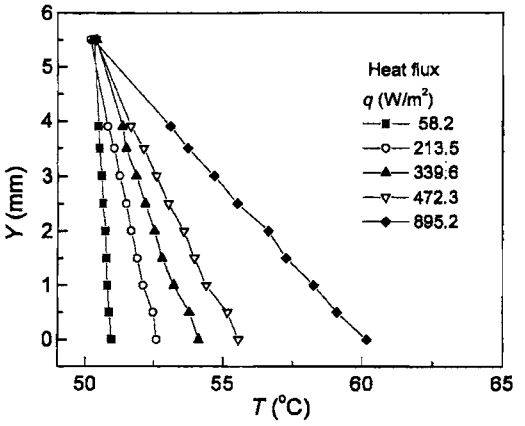

Fig. 13 Vertical fluid temperature distribution in the middle of enclosure at the thermal steady conditions for AR=21.8 or H=5.5 mm, C_m=20%, and the PCM in the slurry is in liquid phase.

5. Steady Convection Heat Transfer in the Microemulsion PCM Slurry

5.1 Effect of aspect ratio

The previous preliminary numerical analysis showed that the PCM could enhance natural convection heat transfer, because of its great latent heat capacity near the heating or cooling boundaries[17]. It is the phase changing process rather than the density variation responsible for the heat transfer enhancement. Because a high temperature difference can be maintained near the thermal boundaries due to the phase change of PCM that a relatively large heat transfer coefficient can be obtained.

Figure 14 shows the Nusselt number against the Rayleigh number for the enclosures with various aspect ratios and for the PCM slurry at a mass concentration of 20%. By increasing the enclosure height, the Rayleigh number is increased at the same temperature difference. As shown in Fig. 14, the onset point had not been observed for AR=10.5 and 4.9, because convection was induced at the very beginning of the experiment. However, the decrease in Nusselt number while the heating plate temperature was over 46°C had been observed for all of the configurations.

According to the latest experimental results[18] by the authors, the Nusselt number did not show a monotonic increasing relationship with the Rayleigh number while the height of the enclosure (the width was fixed) was increased. A conduction lid could be induced at the upper most top of the enclosure if its

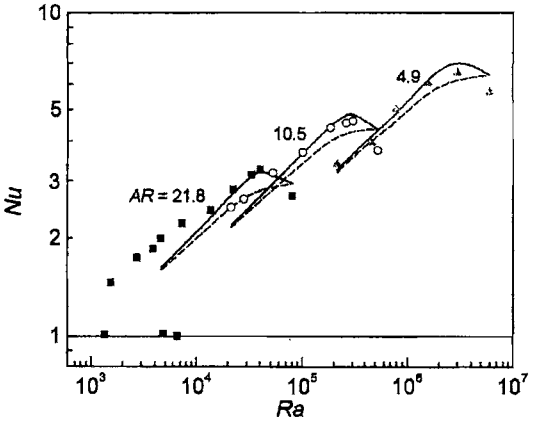

Fig. 14 Nusselt number vs Rayleigh number at thermal steady state conditions for various height enclosures (AR=21.8(■), 10.5(○) and 4.9(▲)) and C_m=20%. Solid lines are the calculated using Eq. (7), and they converts to dash lines if not considering the *Ste* term.

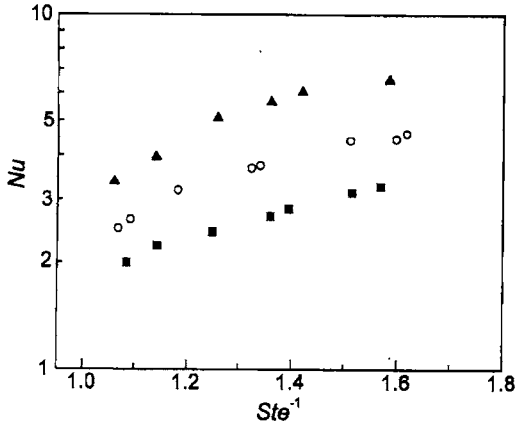

Fig. 15 Nusselt number again inverse Stefan number at thermal steady state conditions for various height enclosures (AR=21.8(■), 10.5(○) and 4.9 (▲)) and C_m=20%. The PCM is in phase changing.

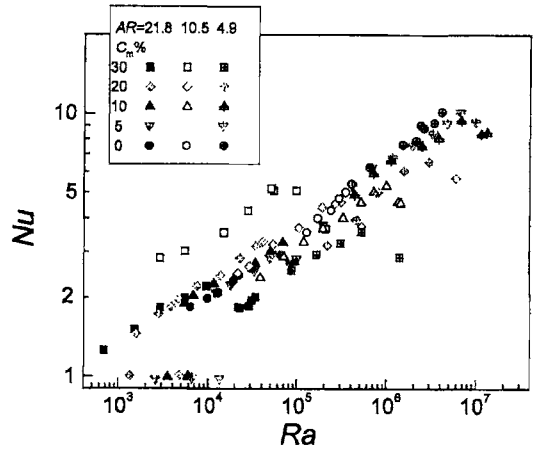

Fig. 16 Nusselt numbers against Rayleigh numbers for the PCM in phase changing at various mass concentrations and enclosures

height is over a limitation[18].

5.2 Effect of Stefan number

It is considered that there appears the local maximum Nusselt number while the PCM generates the latent heat in a phase changing during natural convection in the enclosure. Therefore, a modified Stefan number was introduced for the correlation of experimental data. The definition of Stefan number is as follows:

$$Ste=\frac{C_{p0}(T_H-T_C)}{\int_{T_C}^{T_H} C_p\,dT} \qquad (5)$$

Where the specific heat C_{p0} was taken at temperature of 40°C. C_p is the apparent specific heat. In fact, the modified Stefan number is the ratio of sensible heat of the slurry without PCM to the total heat including latent heat with PCM. The later is an integrally averaged for the PCM slurry in the phase changing region from T_C to T_H. Figure 15 shows the Nusselt number against the reciprocal of Stefan number for the same data shown in Fig. 14. A close relationship between Nu and Ste has been observed from Fig. 15.

5.3 A general correlation

In order to give a general correlation for the Rayleigh-Bénard convection in the PCM microemulsion slurry, various experiments had been conducted. The mass concentration of the PCM was varied from 5% to 30%, and the aspect ratio AR from 21.9 to 4.9. The natural convections both with and without phase changing process had been considered. Figure 16 shows the Nusselt numbers against the Rayleigh numbers at various mass concentrations and aspect ratios for the PCM in phase changing. The correlations of Nu with respect to Ra, AR, n and C_m for the PCM in solid phase, phase changing and liquid phase, can be obtained.

For PCM in solid phase (T_H=30 - 40°C, T_C=30°C)

$$Nu=0.22(1-2.7C_m e^{-0.063AR})Ra^{1/(3n+1)} \qquad (6)$$

where $Ra=1.5\times10^3$ - 6.0×10^6, AR=5.0 - 21.8 and C_m =5 - 30%.

For PCM in phase changing (T_H=40 - 50°C, T_C= 40°C)

$$Nu=0.22(1-3.0C_m e^{-0.03AR})Ra^{1/(3n+1)}Ste^{-1/4} \qquad (7)$$

where $Ra=7.0\times10^2$ - 2.0×10^7, Ste=0.5 - 1, AR=5.0 - 21.8 and C_m=5 - 30%. While T_H>50°C, Ste is given as unity. Since it is believed that the effect of phase change on heat transfer can be negligible in this case.

For PCM in liquid phase (T_H=50 - 65°C, T_C= 50°C)

$$Nu=0.22(1-2.0C_m e^{-0.02AR})Ra^{1/(3n+1)} \qquad (8)$$

where $Ra=2.0\times10^3$ - 5.0×10^6, AR=5.0 - 21.8 and C_m =5 - 30%.

Except for the modified Stefan number in Eq.(7), the differences among the three correlations above are the constant multipliers of C_m and AR. These constants were obtained by fitting the experimental data in various cases with the least-square method. After that they were rounded with one decimal point. It is shown that the multiplier of AR (=0.063) for Eq.(6) is the largest among the three indicating the largest sidewall influence on natural convection due to slurry viscosity. However, the multiplier of C_m for Eq.(7) is the largest (=3.0). This results in the lowest value of the parenthesis term comparing with those of Eq. (6) and Eq.(8) for the same C_m and AR. The main reason is considered to be the great variation in fluid properties in the phase changing temperature range. Note that the pseudoplastic fluid index n included in the correlations also varies dramatically with temperature in the phase changing temperature range. For C_m=20%, AR=5, the same Ra and n, as an example,

without considering the latent heat effect, the Nusselt number for the PCM in phase changing is about 12% and 15% lower than those for the PCM in solid and liquid phase, respectively. Considering the latent effect, the values become 6%, and 9%, respectively. It is acknowledged that the correlation form is not perfect. For example, in the case of $C_m=0$ (water), the value in the parenthesis becomes unity no matter what the aspect ratio AR is, and the Eqs.(6) - (8) reduce to $Nu=0.22Ra^{1/4}$.

The effect of phase change on heat transfer can be evaluated according to Eq.(7) by including the *Ste* term or not. As shown in Fig. 14 for the case $C_m=$ 20%, phase changing process always has a positive effect on heat transfer that the solid lines are located over the dash lines. The greatest difference between the Nusselt numbers for the cases with and without phase changing appears at a heating plate temperature of about 46°C, since at this temperature the *Ste* number reaches its maximum.

The standard deviation for all of the experimental data using the correlation is about ±9%. The standard deviations are ±5.4%, ±11.2% and ±13.2%, respectively, for the PCM in a solid phase, phase changing and a liquid phase. The uncertainties in the measured Rayleigh number and Nusselt number are estimated to be 4% and 3%, respectively.

6. Concluding Remarks

In the present experiments, the onset and convective stability problem in microemulsion PCM slurry for a Rayleigh-Bénard configuration were investigated. The thermal conditions of the experimental system were monitored continuously from a motionless conductive state to a natural convective state by increasing the heating rate through the fluid layer in step. Some hydrodynamic and heat transfer characteristics at the onset point and deflection point in the phase changing region have been obtained. According to our experimental results, the following conclusions can be drawn:

1. Hysteresis phenomenon of *Nu* with respect to *Ra* may exist for Rayleigh-Bénard convection in microemulsion PCM slurry, either the PCM in a single solid phase or in phase changing. The reason for this is not yet clear.

2. If a hysteresis phenomenon exists, the fluid temperature at the center of enclosure undergoes a time-dependent fluctuation while the fluid layer changing from a thermal conductive state to a convective state.

3. The onset of convection seems to be induced easier for the PCM in phase changing compared with that for the PCM in a solid phase, and the critical Rayleigh number decreases with increasing the PCM mass concentration in the range from 5% to 30%.

4. There is a local maximum Nusselt number in a *Nu-Ra* plot for the PCM in phase changing, and the flow pattern is quite unstable while the heating plate temperature is higher than the temperature in which the fluid has its maximum apparent specific heat. Corresponding to the decrease in Nusselt number with respect to Rayleigh number, a deflection point exists for the heating plate temperature with time while the lower heating plate being heated under a constant heat flux.

References

(1) Chandrasekhar, S., Hydrodynamic and Hydromagnetic Stability, (1961), Oxford University Press.

(2) Davis, S.H., The Stability of Time Periodic Flows, Ann. Rev. Fluid Mech., Vol. 8 (1976), pp. 57-74.

(3) Manneville, P., Dissipative Structures and Weak Turbulence, (1990), Academic Press.

(4) Getling, A.V., Rayleigh-Bénard Convection: Structures and Dynamics, (1998), World Scientific.

(5) Cerisier, P., Rahal, S., Cordonnier, J. and Lebon, G., Thermal Influence of Boundaries on the Onset of Rayleigh-Bénard Convection, Intl. J. Heat Mass Transfer, Vol. 41 (1998), pp. 3309-3320.

(6) Howle, L.E., The Effect of Boundary Properties on Controlled Rayleigh-Bénard Convection, J. Fluid Mech., Vol. 411 (2000), pp. 39-58.

(7) Ang, J. and Bau, H.H., Experiments on the Stabilization of the No-Motion State of a Fluid Layer Heated from Below and Cooled from Above, J. Fluid Mech., Vol. 363 (1998), pp. 153-171.

(8) Howel, L.E., Active Control of Rayleigh-Bénard Convection, Phys. Fluids, Vol. 9 (1997), pp. 1861-1863.

(9) Chung, C.A. and Chen, F., Onset of Plume Convection in Mushy Layers, J. Fluid Mech., Vol. 408 (2000), pp. 53-82.

(10) Lehn, J.M., Toward Self-Organization and Complex Matter, Science, Vol. 295 (2002), pp. 2400-2402.

(11) Ikkala, O. and Brinke, G.T., Functional Materials Based on Self-Assembly of Polymeric Supramolecules, Science, Vol. 295 (2002), pp. 2407-2409.

(12) Chen, K. and Ma, Y.Q., Self-Assembling Morphology Induced by Nanoscale Rods in a Phase-Separating Mixture, Phys. Rev. E., Vol. 65 (2002), pp. 492-501.

(13) Yamamoto, J. and Tanaka, H., Transparent Nematic Phase in a Liquid-Crystal-Based Microemulsion, Nature, Vol. 409 (2001), pp. 321-325.

(14) Inaba, H., New Challenge in Advanced Thermal Energy Transportation Using Functionally Ther-

mal Fluids, Int. J. Therm. Sci., Vol. 39 (2000), pp. 991-1003.
(15) Choi, E., Cho, Y.I. and Lorsch, H.G., Forced Convection Heat Transfer with Phase-Change-Material Slurries: Turbulent Flow in a Circular Tube, Intl. J. Heat Mass Transfer, Vol. 37 (1994), pp. 207-215.
(16) Inaba, H. and Morita, S., Flow and Cold Heat-Storage Characteristics of Phase-Change Emulsion in a Coiled Double-Tube Heat Exchanger, ASME J. Heat Transfer, Vol. 117 (1995), pp. 440-446.
(17) Inaba, H., Dai, C. and Horibe, A., Numerical Simulation of Rayleigh-Bénard Convection in Non-Newtonian Phase-Change-Material Slurries, Intl. J. Thermal Sciences, Vol. 42 (2003), pp. 271-480.
(18) Inaba, H., Dai, C. and Horibe, A., Natural Convection Heat Transfer in Enclosures with Microemulsion Phase Change Material Slurry, (in Japanese), Proceedings of 39th National Heat Transfer Symposium of Japan, E234, (2002), pp. 481-482.
(19) Datta, P., Sengupta, S. and Singh, T., Rayleigh and Prandtl Number Effects in Natural Convection in Enclosures with Microencapsulated Phase Change Materials Slurries, The 33rd Symposium on Heat Transfer of Japan, (1996), pp. 225-226.
(20) Rothstein, J.P. and Mckinley, G.H., Non-Isothermal Modification of Purely Elastic Flow Instabilities in Torsional Flows of Polymeric Fluids, Phys. Fluids, Vol. 13, No. 2 (2001), pp. 382-396.
(21) Ali, M.E., Hydrodynamic Stability of a Suspension in Cylindrical Couette Flow, Phys. Fluids, Vol. 14 (2002), pp. 1236-1243.
(22) Davis, S.H., Convection in a Box: Linear Theory, J. Fluid Mech., Vol. 30 (1967), pp. 465-478.
(23) Stork, K. and Müller, U., Convection in Boxes: Experiments, J. Fluid Mech., Vol. 54 (1972), pp. 599-611.
(24) Ozoe, H. and Churchill, S.W., Hydrodynamic Stability and Natural Convection in Ostwald-de Waele and Ellis Fluids: The Development of a Numerical Solution. AIChE Journal, Vol. 18, No. 8 (1972), pp. 1196-1206.
(25) Tien, C., Tsuei, H.S. and Sun, Z.S., Thermal Instability of a Horizontal Layer of Non-Newtonian Fluid Heated from Below, Intl. J. Heat Mass Transfer, Vol. 12 (1969), pp. 1173-1185.
(26) Parmentier, E.M. and Turcotte, D.L., Studies of Finite Amplitude Non-Newtonian Thermal Convection with Application to Convection in the Earth Mantle, J. Geophysical Research, Vol. 81 (1976), pp. 1839-1846.
(27) Solomatov, V.S., Scaling of Temperature-and Stress-Dependent Viscosity Convection, Phys. Fluid, Vol. 7 (1995), pp. 266-274.
(28) Bottaro, A., Metzener, P. and Matalon, M., Onset and Two-Dimensional Patterns of Convection with Strongly Temperature-Dependent Viscosity, Physics of Fluids, Vol. 4 (1992), pp. 655-663.
(29) Slavtchev, S. and Ouzounov, V., Stationary Marangoni Instability in a Liquid Layer with Temperature-Dependent Viscosity in Microgravity, Microgravity Quarterly, Vol. 4 (1994), pp. 33-38.
(30) Selak, R. and Lebon, G., Rayleigh-Marangoni Thermoconvective Instability with Non-Boussinesq Corrections, Internat. J. Heat Mass Transfer, Vol. 40 (1997), pp. 785-798.
(31) Richter, F.M., Nataf, H.C. and Daly, S.F., Heat Transfer and Horizontally Averaged Temperature of Convection with Large Viscosity Variations, J. Fluid Mech., Vol. 129 (1983), pp. 173-192.
(32) Thess, A. and Orszag, S.A., Surface-Tension-Driven Bénard Convection at Infinite Prandtl Number, Journal of Fluid Mechanics, Vol. 283 (1995), pp. 201-230.
(33) Hollands, K.G.T., Raithby, G.D. and Konicek, L., Correlation Equation for Free Convection Heat Transfer in Horizontal Layers of Air and Water, Internat. J. Heat Mass Transfer, Vol. 18 (1975), pp. 879-884.
(35) Busse, F.H., The Oscillatory Instability of Convection Rolls in a Low Prandtl Number Fluid, J. Fluid Mechanics, Vol. 52, No. 1 (1972), pp. 97-112.
(35) Booker, J.R., Thermal Convection with Strongly Temperature-Dependent Viscosity, J. Fluid Mech., Vol. 76 (1976), pp. 741-754.
(36) Stengel, K.C., Oliver, D.S. and Booker, J.R., Onset of Convection in a Variable-Viscosity Fluid, J. Fluid Mech., Vol. 120 (1982), pp. 411-431.
(37) Ogawa, M., Schubert, G. and Zebib, A., Numerical Simulations of Three-Dimensional Thermal Convection in a Fluid with Strongly Temperature-Dependent Viscosity, J. Fluid Mech., Vol. 233 (1991), pp. 299-328.
(38) Christensen, U., Convection in a Variable-Viscosity Fluid: Newtonian Versus Power-Law Rheology, Earth and Planetary Science Letters, Vol. 64 (1983), pp. 153-162.